



Repositorio Institucional de la Universidad Autónoma de Madrid

<https://repositorio.uam.es>

Esta es la **versión de autor** del artículo publicado en:

This is an **author produced version** of a paper published in:

PHYSICAL CHEMISTRY CHEMICAL PHYSICS 20.4 (2018): 2413-2420

DOI: <http://doi.org/10.1039/C7CP07891A>

Copyright: © 2018 The Owner Societies

El acceso a la versión del editor puede requerir la suscripción del recurso
Access to the published version may require subscription

Alkaline-earth (Be, Mg, Ca) bonds at the origin of huge acidity enhancements.

M. Merced Montero-Campillo,^b Pablo Sanz,^a Otilia M^o,^a Manuel Y^añez,^{a,*} Ibon Alkorta^{b*} and Jos^e Elguero.^b

^aDepartamento de Quⁱmica, Facultad de Ciencias, M^odulo 13, and Institute of Advanced Chemical Sciences (IadChem), Universidad Aut^onoma de Madrid. Campus de Excelencia UAM-CSIC, Cantoblanco, 28049-Madrid. Spain

^bInstituto de Quⁱmica M^edica, CSIC, Juan de la Cierva, 3, 28006 Madrid. Spain

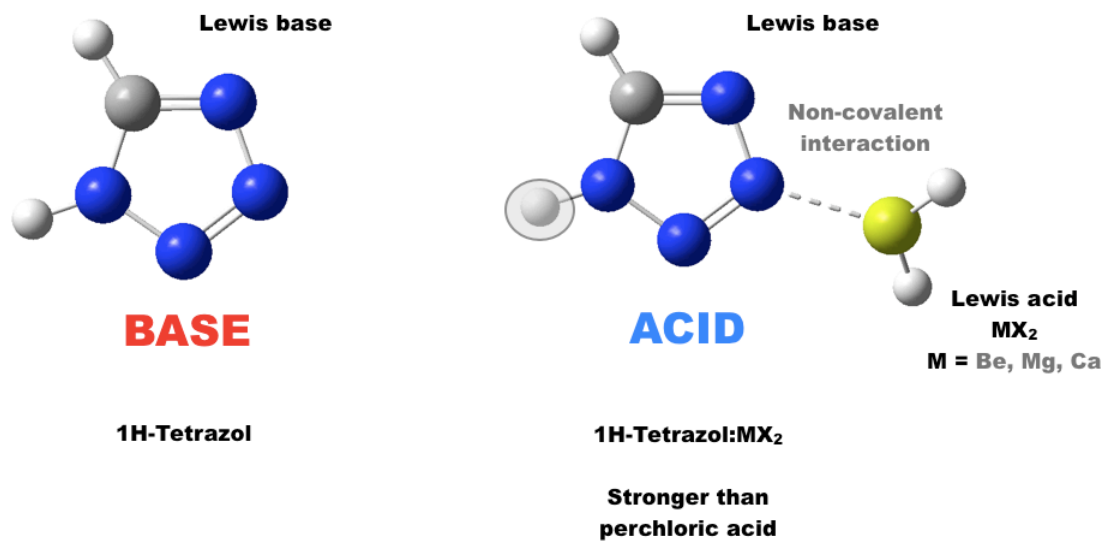
*e-mail: manuel.yanez@uam.es; ibon@iqm.csic.es

Abstract

The interaction between alkaline-earth derivatives of general formula X_2M ($X = H, F, Cl$; $M = Be, Mg, Ca$) and a set of Lewis bases including first and second-row hydrides, namely YH_n ($Y = O, N, F, S, P, Cl$) hydrides, as well as other typical cyclic organic bases such as aniline, 1H-1,2,3-triazole, 1H-tetrazole and phenylphosphine, was investigated at the G4 *ab initio* composite method. Contrary to what might be expected, it was found that the interactions involving Mg and Ca derivatives are not necessarily weaker than those with beryllium bonds. The origin is two-folded, the larger deformation of the interacting systems when Be-derivatives are involved, and the appearance of secondary non-covalent interactions in the formation of some of the Mg- and Ca-containing complexes. Hence, the dissociation of the latter complexes may require higher enthalpies than the Be ones. These deformations are triggered by a significant redistribution of the electron density of the two interacting moieties, which also result in dramatic changes of the reactivity of the interacting compounds and in particular on the intrinsic basicity of the Lewis bases investigated, to the point that conventional bases such as ammonia or aniline, upon complexation with MCl_2 ($M = Be, Mg, Ca$), become stronger Br \ddot{o} sted acids than phosphoric acid, whereas other bases such as 1H-tetrazole become stronger acids than perchloric acid.

Keywords: Beryllium bonds; Magnesium bonds; Calcium bonds; deformation energy; basicity enhancement; *ab initio* calculations

Graphical Abstract



Upon association with MX_2 ($\text{M} = \text{Be}, \text{Mg}, \text{Ca}$) alkaline-earth derivatives conventional bases become very strong acids.

1. Introduction

The intermolecular interactions involving closed-shell systems play a significant role in many chemical processes. Perhaps the most paradigmatic example is that of hydrogen bonds,¹ which are responsible for the macroscopic properties of very simple compounds, such as water, and for the characteristics of very complicated assemblies such as DNA. In the last decades, a pleiad of other closed-shell interactions,² namely dihydrogen bonds,^{3,4} halogen bonds,⁵ tetrel bonds,⁶⁻⁸ pnictogen bonds⁹, chalcogen bonds¹⁰⁻¹² and beryllium bonds¹³ have been described in the literature, which obey to a common bonding scheme based on the Lewis pair concept. The interaction within this pair automatically implies certain electron density redistribution between the Lewis base (LB) and Lewis acid (LA) subunits. Therefore, the larger these perturbations of the electron density, the stronger the interaction, what lately results into a dramatic change on the intrinsic properties of the interacting systems. For instance, we have shown that conventional bases can be changed into gas-phase superacids¹⁴ through the formation of complexes with Be derivatives, and that a spontaneous proton transfer occurs when a beryllium derivative interacts with a hydrogen bonded complex.¹⁵ Similarly, beryllium bonds can modulate the strength of other non-covalent interactions, such as halogen bonds. Indeed, it is possible in this way to change conventional halogen-bonded complexes into halogen-shared or even ion-pair complexes.¹⁶ More recently, it has also been shown that the aforementioned electron density redistributions triggered by the formation of beryllium bonds can lead to the exergonic and spontaneous formation of radicals,¹⁷ and may be also the base to design anion-sponges.^{18,19}

It is quite obvious that the perturbation produced when a BeXY moiety, acting as a Lewis acid, interacts with a Lewis base, is rather strong due to the electron deficient nature of Be. All the other alkaline-earth elements of the group are expected to share this electron deficient nature, since they have a same valence shell structure. In agreement with this, we recently showed that MgX₂ derivatives also yield complexes with first- and second-row Lewis bases stabilized by the formation of magnesium bonds.²⁰

Taking into account that the main limitation of tailoring properties by beryllium bonds is the huge toxicity of beryllium and its derivatives, it becomes crucial to know whether the complexation with magnesium or calcium derivatives can be an alternative to the use of beryllium compounds. In other words, we intend along this paper to

answer questions such as what is the strength of magnesium or calcium bonds with respect to beryllium ones, how large are perturbations induced in the Lewis base electron density upon interaction through a magnesium or a calcium bond with respect to beryllium bonds and, finally, what are the effects of these interactions on the intrinsic properties of the Lewis base and in particular on its intrinsic acidity. With these purposes in mind, we investigate in this paper, through the use of high-level *ab initio* calculations, the structure and stability of $X_2M:LB$ ($X = H, F, Cl$; $M = Be, Mg, Ca$) where the set of LBs includes the YH_n ($Y = O, N, F, S, P, Cl$) hydrides of the first and the second row, as well as the following organic bases: aniline, 1H-1,2,3-triazole, 1H-tetrazole and phenylphosphine, as paradigmatic examples of good organic bases.

2. Computational Details

In order to obtain reliable results in our comparison of beryllium, magnesium and calcium bonds, we will use the high-level *G4 ab initio* formalism.²¹ This composite method is based on B3LYP optimized geometries, through the use of 6-31G(2df,p) basis set expansion for first- and second-row atoms and 6-31G(2fg,p) for third-row no transition metal elements. The same level of theory is used to calculate the harmonic vibrational energies and the thermochemical corrections to the total enthalpy or free energy. Correlation effects are accounted for by using Moller-Plesset perturbation theory up to the fourth-order and coupled cluster theory. A further correction is added to the resulting energy by extrapolating to the Hartree-Fock limit using quadruple-zeta and quintuple-zeta basis sets. The overall average absolute deviation estimated for energies obtained by this procedure is 3.5 kJ/mol.²¹

The binding enthalpies of the $X_2M:LB$ complexes investigated, D_0 , were calculated as the enthalpy difference between the isolated X_2M and LB compounds and that of complex they form. The intrinsic acidity of these complexes was obtained as the enthalpy difference between the neutral and the deprotonated complex. To the value so obtained, a constant contribution of 6.2 kJ.mol⁻¹ was added, which corresponds to the (5/2)RT factor which accounts for the translational energy of the proton and the (PV) term.

The bonding of the systems under investigation was analyzed through the use of two different approaches, namely the quantum theory of atoms in molecules (QTAIM),²² the electron localization function (ELF).²³ The QTAIM offers an

interpretation of bonding based on a topological analysis of the electron density by locating the maxima (nuclear attractors) and other critical points (bond, ring and cage critical points, abbreviated as BCP, RCP and CCP) and the paths of minimum gradients connecting them. These calculations were carried out with the AIMAll program.²⁴ The ELF function allows a partition of the molecular space in monosynaptic and disynaptic (or polysynaptic) basins. The first ones are associated with core electrons and/or lone pairs, whereas the second ones correspond to bonding regions. The ELF function was obtained with the Topmod package.²⁵

Alkaline-earth bonds were also characterized by analyzing the characteristics of low-reduced gradient regions usually associated to low-density values through the use of the NCIPLOT program, where NCI stands for non covalent interactions.²⁶ The isosurfaces associated to these NCI regions are plotted using a color code associated to the sign of the second eigenvalue of the electron-density Hessian. In this color code, blue stands for strong attractive NCI, red stands for strong repulsive NCI, and weak interactions within the van der Waals range appear in green.

3. Results and Discussion.

3.1. X₂M:LB complexes stability.

We summarized in Table 1 the G4 binding enthalpies of the complexes X₂M:LB (X = H, F, Cl; M = Be, Mg, Ca; LB = NH₃, H₂O, FH, PH₃, SH₂, ClH), defined in the usual way, i.e., the enthalpy of the complex minus the enthalpies of the two interacting systems, when both complexes and isolated compounds in their equilibrium conformations. In Table 1 we also report the corresponding interaction enthalpies, defined as the stabilization of the complex with respect to the two interacting systems, with the geometry they have in the complex. Obviously the difference between binding and interaction enthalpies measures the enthalpy necessary to deform both interacting systems, also reported in Table 1.

Table 1. G4 binding enthalpies (D_0), interaction enthalpies (E_{int}) and deformation enthalpies (E_{def}) for complexes formed between different Lewis bases and MH_2 , MF_2 , MCl_2 ($M = \text{Be, Mg, Ca}$) Lewis acids. All values in kJ mol^{-1} .

	D_0			E_{int}			E_{def}		
	Be	Mg	Ca	Be	Mg	Ca	Be	Mg	Ca
MH_2-NH_3	-95	-77	-87	-124	-87	-87	29	10	0
MH_2-H_2O	-76	-68	-95	-101	-75	-110	25	7	15
MH_2-FH	- ^a	- ^a	- ^a	- ^a	- ^a	- ^a	- ^a	- ^a	- ^a
MH_2-PH_3	-31	-27	-40	-51	-33	-41	20	6	1
MH_2-SH_2	-32	-31	- ^a	-47	-34	- ^a	15	3	- ^a
MH_2-CIH	-13	- ^a	- ^a	-18	- ^a	- ^a	5	- ^a	- ^a
MF_2-NH_3	-114	-114	-88	-157	-126	-88	43	12	0
MF_2-H_2O	-90	-100	-93	-125	-110	-96	35	10	3
MF_2-FH	-38	-76	-104	-58	-119	-241	20	43	136
MF_2-PH_3	-38	-52	-44	-66	-64	-44	28	12	0
MF_2-SH_2	-41	-57	-52	-64	-63	-52	23	6	0
MF_2-CIH	-22	-80	-112	-30	-435	-364	8	355	252
MCl_2-NH_3	-125	-118	-96	-176	-133	-102	51	15	6
MCl_2-H_2O	-97	-102	-89	-143	-114	-98	46	12	9
MCl_2-FH	-36	-62	-72	-68	-78	-90	32	16	18
MCl_2-PH_3	-45	-56	-47	-90	-71	-56	45	15	9
MCl_2-SH_2	-45	-59	-50	-82	-68	-57	37	9	7
MCl_2-CIH	-19	-43	-53	-42	-51	-79	23	8	26

^a Complex not found because the interaction between the Lewis acid and the Lewis base leads to a spontaneous loss of H_2 .

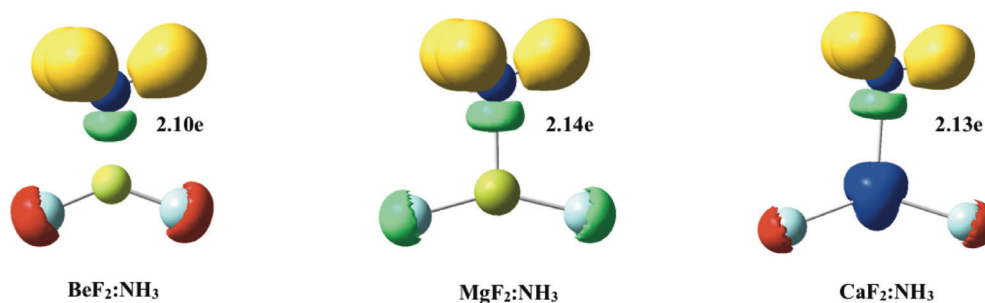


Figure 1. Three-dimensional ELF plots ($ELF = 0.85$) for the $MF_2:NH_3$ complexes. Green and yellow lobes correspond to disynaptic basins involving only heavy atoms and heavy and hydrogen atoms, respectively. Red and blue lobes correspond to monosynaptic basins associated with lone-pairs and core electrons, respectively. The population of the basins is in e.

Looking at Table 1 and Figure S1, the first conspicuous fact is that the calculated binding enthalpies are rather similar for the three alkaline-earth systems considered, indicating that the strength of Be, Mg and Ca bonds is pretty much the same. Consistently, the interaction between the alkaline-earth metal ($M = \text{Be, Mg, Ca}$) and the Lewis base described by the ELF analysis is characterized by the presence of a disynaptic basin with a very similar population ($\sim 2.1e$), as exemplified in Figure 1 for the particular case of $LB = NH_3$.

However, although one should expect Be derivatives to exhibit stronger interactions than their Mg and Ca-analogues, rather unexpectedly, in several cases, the complexes involving Mg and Ca derivatives present larger binding enthalpies. For instance, the binding enthalpies of the $\text{BeF}_2\cdot\text{NH}_3$ and the $\text{MgF}_2\cdot\text{NH}_3$ complexes are equal, whereas those of the $\text{MgF}_2\cdot\text{H}_2\text{O}$ and $\text{CaF}_2\cdot\text{H}_2\text{O}$ systems are larger, in absolute value, than that of $\text{BeF}_2\cdot\text{H}_2\text{O}$. This gap seems to be even more pronounced when dealing with second-row Lewis bases. As shown in Table 1, the binding enthalpies of the complexes between MgF_2 and CaF_2 with PH_2 , SH_2 and ClH are always larger, in absolute value, than those with BeF_2 . The effect is particularly dramatic precisely in the $\text{CaF}_2\cdot\text{ClH}$ case, where the binding enthalpy is five times larger than that of $\text{BeF}_2\cdot\text{ClH}$ (-112 vs -22 kJ/mol).

There are two main factors behind these unexpected results, the extent of the deformation of the Lewis acid upon formation of the complex and the role of secondary non-covalent interactions. Let us explain in detail these two phenomena. As it was pointed out in the seminal article describing beryllium bonds,¹³ these interactions involve a strong deformation of the BeX_2 moiety triggered by the strong polarization of the lone pairs of the Lewis base towards both the empty p orbital of the metal and the $\sigma^*_{\text{Be-X}}$ antibonding orbitals. As a consequence of this polarization the initially empty p orbital of Be becomes slightly populated leading to a change of its hybridization from sp , in the isolated molecule, to sp^2 in the complex, which results in a significant departure from linearity of the BeX_2 molecule. The second charge transfer towards the $\sigma^*_{\text{Be-X}}$ anti-bonding orbitals leads to a non-negligible lengthening of the BeX bonds in the complex with respect to the isolated molecule. The same polarization effects, although weaker, are also observed when magnesium and calcium bonds are formed, leading to similar geometry changes (see Figure 2).

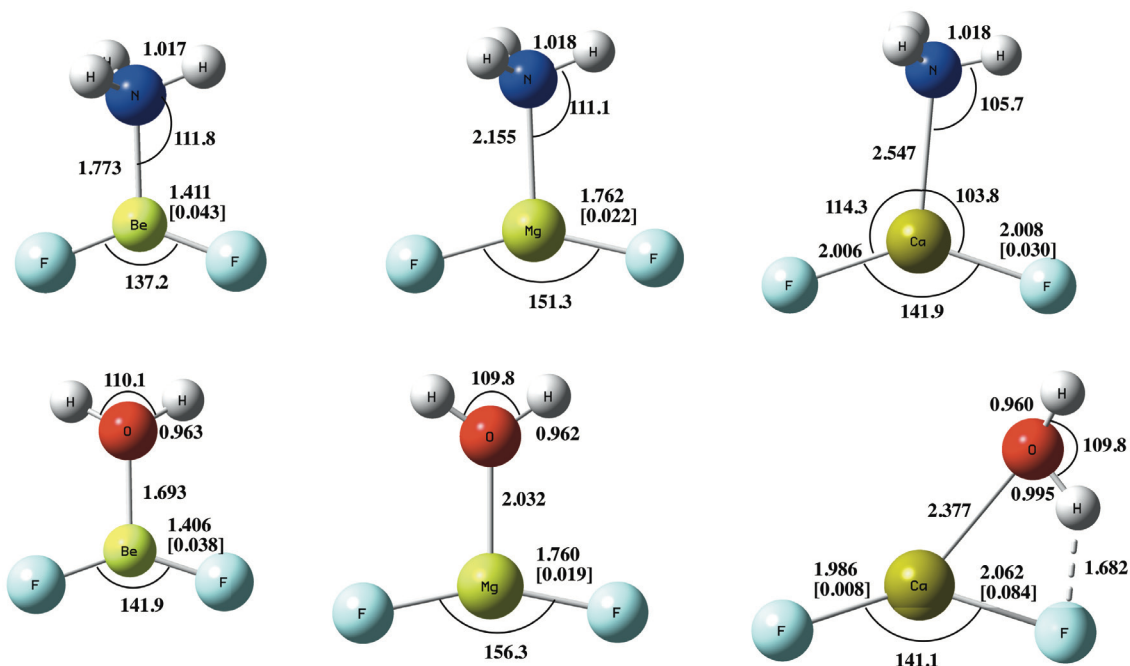


Figure 2. G4 Optimized structures of the complexes formed upon interaction of MF₂ (M = Be, Mg, Ca) derivatives with ammonia and water. Bond angles in degrees and bond lengths in Å. The values within square brackets indicate the lengthening of the M–F bond (M = Be, Mg, Ca) on going from the isolated MF₂ molecule to the MF₂:LB (LB = NH₃, H₂O) complex.

Indeed, it is apparent that the MgF₂ in the complex with ammonia also becomes bent but to a lesser degree than BeF₂ does. In the case of the complex with CaF₂, the isolated molecule is already bent, with a F–Ca–F angle of 135.2°, which becomes slightly wider in the complex due to a H···F NCI which is reflected in the slight tilt of the ammonia molecule. Also, the lengthening of the Mg–F and the Ca–F bonds is smaller than that calculated for the Be–F bonds, indicating that, as expected, the interactions of ammonia with MgF₂ and CaF₂ are weaker than with BeF₂. These geometrical findings are consistent with the changes observed in the electron densities. As illustrated in Figure 3, in all cases the electron density at the M–F (M = Be, Mg, Ca) BCP decreases on going from the isolated molecules to the complex, and this decrease is always significantly larger for the BeF₂ containing systems. There is also one strong H···F hydrogen bond in CaF₂:H₂O, with the concomitant weakening of the O–H and the Ca–F bonds participating in this non-covalent interaction.

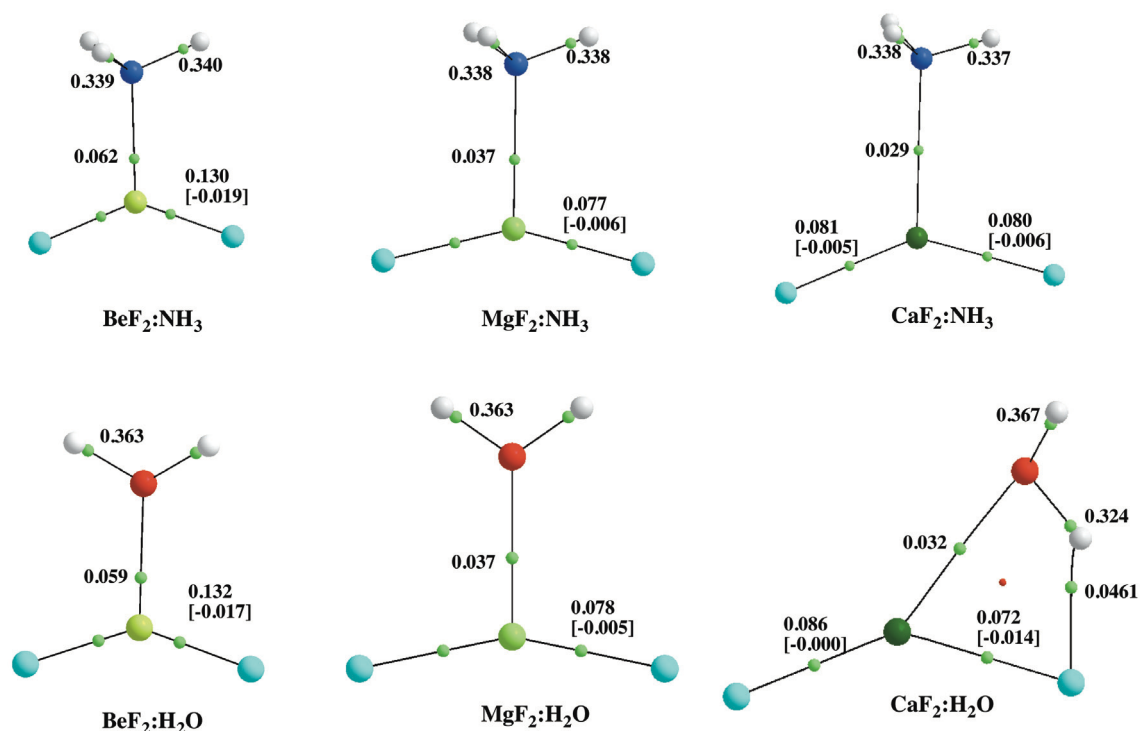


Figure 3. Molecular graphs of the $\text{MF}_2\text{:NH}_3$ and $\text{MF}_2\text{:H}_2\text{O}$ complexes ($\text{M} = \text{Be}, \text{Mg}, \text{Ca}$). Green and red dots denote BCPs and RCPs, respectively. The electron densities at the BCPs are given in a.u. The values within brackets show the decrease in the density at the corresponding BCPs on going from the isolated MF_2 molecule to the MF_2 molecule in the complex

Why the aforementioned trends are apparently not reflected in the corresponding binding enthalpy of the complexes can be understood if we consider the balance between interaction and deformation enthalpies rather than binding enthalpies. Considering the $\text{MF}_2\text{:NH}_3$ complexes (Table 1), the absolute value of the interaction enthalpies, E_{int} , decrease in the order $\text{Be} > \text{Mg} > \text{Ca}$ ($157 > 126 > 88 \text{ kJ}\cdot\text{mol}^{-1}$), a trend also followed by the deformation enthalpies ($43 > 12 > 0 \text{ kJ}\cdot\text{mol}^{-1}$). The resulting balance gives a binding enthalpy of -114 kJ/mol for both Be and Mg complexes, hiding a larger interaction enthalpy for the beryllium case. The situation is even more evident as far as the $\text{MF}_2\text{:H}_2\text{O}$ complexes are concerned, because, as mentioned above, the binding enthalpies of both the MgF_2 and the CaF_2 complexes are larger, in absolute value, than that of the BeF_2 analogue. A larger negative charge at the F atom when it is bound to Ca (-0.84) with respect to Be (-0.57), together with a longer Ca–F bond, favors the appearance of the strong $\text{H}\cdots\text{F}$ bond in the $\text{CaF}_2\text{:H}_2\text{O}$ complex we previously described when commenting Figure 3.

A similar scenario explains the surprisingly high binding enthalpies of the $\text{CaF}_2\text{:ClH}$ and $\text{MgF}_2\text{:ClH}$ complexes with respect to $\text{BeF}_2\text{:ClH}$. In these cases, the hydrogen bond between one F atom and the H atom of the ClH moiety is so strong that induces a Cl-H bond cleavage. As a consequence, the hydrogen atom appears to be bound to the F atom of the MF_2 ($M = \text{Mg}, \text{Ca}$) moiety in the complex. This equilibrium structure can be viewed as the interaction between a MFCl ($M = \text{Mg}, \text{Ca}$) moiety and HF, as shown in Figure 4a.

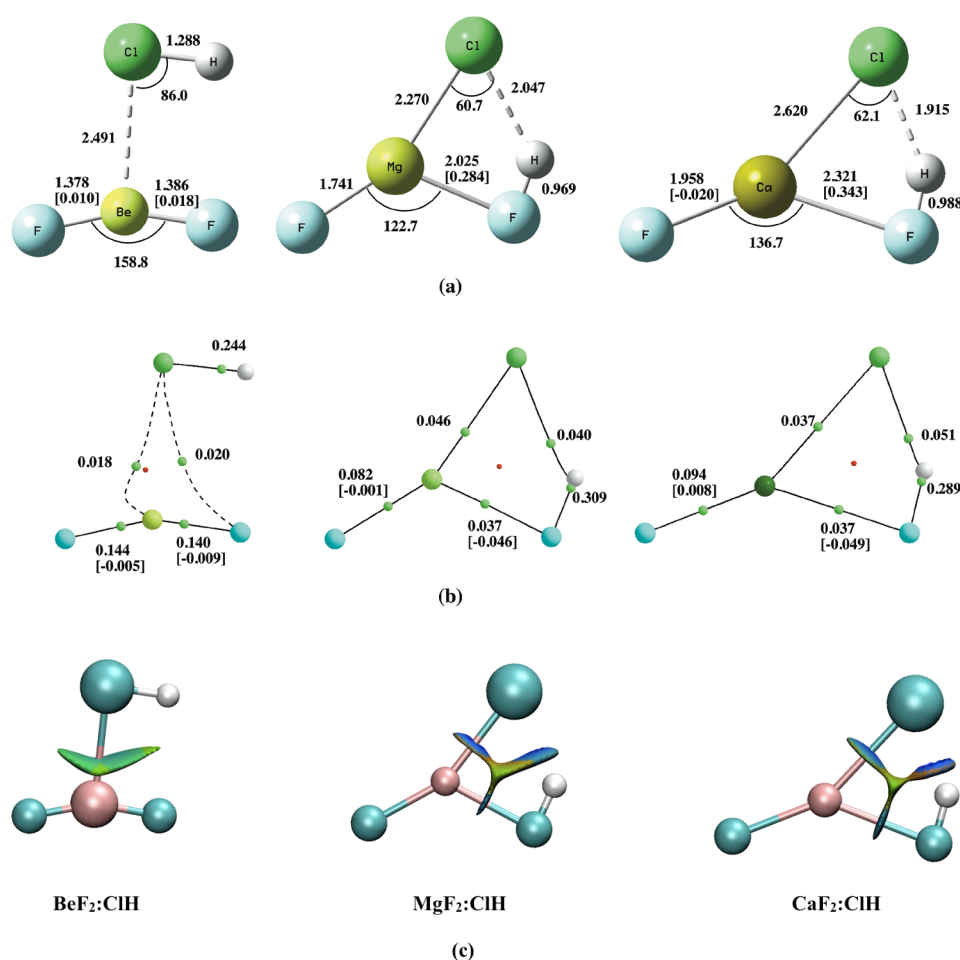


Figure 4. Complexes between MF_2 ($M = \text{Be}, \text{Mg}, \text{Ca}$) derivatives and HCl. (a) Optimized structures. Bond angles in degrees and bond lengths in Å. The values within square brackets indicate the lengthening of the M-F bond ($M = \text{Be}, \text{Mg}, \text{Ca}$) on going from the isolated MF_2 molecule to the $\text{MF}_2\text{:ClH}$ complex. (b) Molecular graphs. Green and red dots denote BCPs and RCPs, respectively. The electron densities at the BCPs are given in a.u.. The values within brackets show the decrease in the density at the corresponding BCPs on going from the isolated MF_2 molecule to the $\text{MF}_2\text{:ClH}$ molecule (c) 3D-NCIPLOT pictures. Blue color stands for strong attractive NCI, whereas red color stands for strong repulsive NCI.

The molecular graph for the Be-containing complex (Figure 4b) shows the existence of a BCP between Cl and one of the F atoms, explaining the elongation of the corresponding Be–F bond and the small Be–Cl–H bond angle, although no BCP associated to a Cl–H···F hydrogen bond is found yet in this case. For the Mg- and Ca-containing complexes, as mentioned before, this hydrogen bond is strong and leads to a complete proton transfer from the ClH molecule to the MF₂ (M = Mg, Ca) moiety. The newly formed F–H bond presents electron densities at the BCP rather close to that of an isolated HF molecule (0.315 a.u.). Accordingly, the Cl–H covalent bond becomes a hydrogen bond that is stronger in the Ca containing complex than in the Mg one, as reflected by a larger electron density at the Cl···H BCP, and a smaller density at the F–H BCP. This AIM description is also coherent with the three-dimensional NCI plots (see Figure 4c), showing an asymmetric Be–Cl lobe for the Be-containing compound, distorted towards the H atom, and a tri-lobate region for the Mg- and Ca-containing complexes associated with the M–Cl and M–F bonds, and the Cl···H hydrogen bond.

A similar proton transfer is observed in complexes between MH₂ (M = Be, Mg, Ca) and HF, but in this case both the M–H and the F–H bond cleave, and the structure found can be seen as a weakly bound complex between a F–M–H (M = Be, Mg, Ca) unit and a H₂ molecule (see Figure S2 of the Supporting Information). The same phenomenon is observed for MgH₂:HCl, CaH₂:HCl and CaH₂:SH₂, also represented in Figure S2.

3.2. Acidity enhancements

As mentioned in the Introduction, one of the signatures of the formation of a beryllium bond is a significant charge transfer from the Lewis base to the electron-deficient beryllium derivative. The most direct consequence is a huge acidity enhancement of the Lewis base, to the point that even conventional Lewis bases such as aniline are changed into superacids.¹⁴ Taking into account that similar effects, even from a quantitative point of view, are found when the system acting as a Lewis acid is a Mg or a Ca derivative as discussed in the previous section, we thought it is clearly justified to investigate whether the formation of complexes with MgX₂ and CaX₂ lead to similar acidity enhancements. For the sake of conciseness, we will discuss only the hydrides and the corresponding chloride derivatives, MX₂ (M = Be, Mg, Ca; X = H, Cl).

We have also considered it of interest in this section to include in our set of Lewis bases typical organic bases such as aniline, 1H-1,2,3-triazole, 1H-tetrazole and phenylphosphine. We summarize in Table 2 the calculated acidities of the different complexes under investigation and those of the corresponding isolated bases, for which experimental acidity values are shown when available.

Table 2. Calculated acidity values of different typical bases and their complexes with MgH₂, MgCl₂, BeH₂ and BeCl₂. All values, unless otherwise indicated, were calculated using the G4 composite high-level *ab initio* method.

Lewis Base	Acidity (free base)	Complex ^a with MH ₂	Complex ^a with MCl ₂
NH ₃	1688.8	1435.0	1373.4
	[1688.0 ± 1.2] ²⁷	1448.9	1390.8
	[1687.7 ± 0.5] ²⁸	1430.6	1399.0
H ₂ O	1629.9	1360.0	1287.8
	[1632.9 ± 0.1] ²⁸	1378.0	1315.5
		1365.4	1317.0
FH	1549.4	- ^b	1162.0
	[1553.649 ± 0.013] ²⁸		1200.0
			1227.5
PH ₃	1539.4	1372.6	1317.5
	[1529.7]	1367.8	1306.5
		1348.7	1320.2
SH ₂	1475.6	1298.3	1243.0
	[1469.81 ± 0.07] ²⁸	1293.8	1235.6
		- ^b	1241.1
ClH	1400.4	1224.0	1159.1
	[1394.876 ± 0.010] ²⁸	- ^b	1150.8
		- ^b	1164.1
Aniline	1537.8	1358.9	1316.4
	[1540.5 ± 1.3] ²⁷	1373.5	1329.2
		1368.0	1350.7
1H-1,2,3-triazole	1431.3	1317.6	1293.9
	[1449. ± 8.8] ²⁷	1328.4	1289.5
		1297.2	1260.3
1H-tetrazole	1380.6	1267.3	1231.0
		1265.6	1230.3
		1228.6	1209.3
Phenylphosphine ^c	1484.8	1372.0	1331.8
		1368.7	1322.7
		1349.2	1329.1

^a Values in the first, second and third rows correspond to M = Be, Mg and Ca, respectively.

^b Complex not found. A spontaneous loss of H₂ takes place.

^c Values calculated at the B3LYP/6-311+G(3df,2p)//B3LYP/6-31+G(d,p) level.

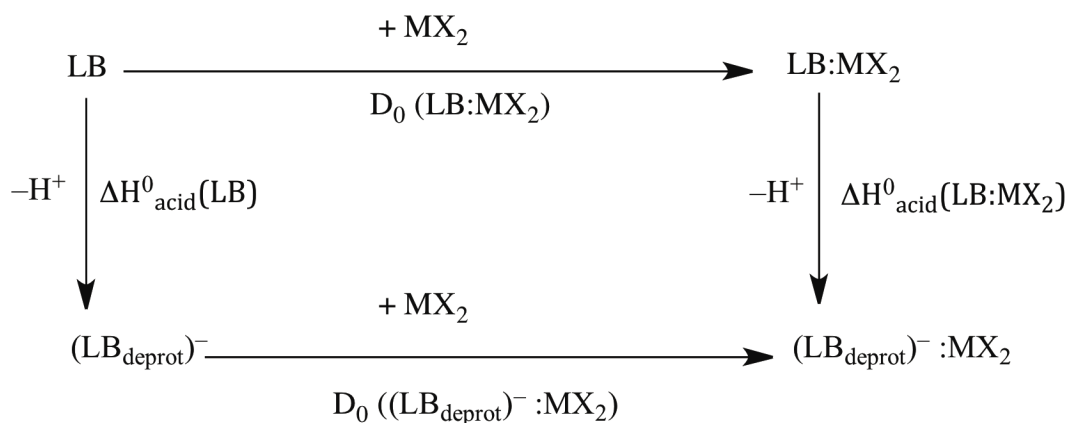
Taking into account that the agreement between our theoretical estimates and the experimental values for the isolated bases is very good, we assume that our calculated values for the complexes with alkaline-earth derivatives are equally reliable. The huge acidity enhancement predicted in all cases is the most important finding that can be

extracted from Table 2. Note that our results predict that a weak acid in the gas phase such as hydrogen sulfide ($\Delta H^0_{\text{acid}} = 1470 \pm 3 \text{ kJ}\cdot\text{mol}^{-1}$)²⁷ becomes a stronger acid than sulfuric acid ($\Delta H^0_{\text{acid}} = 1295 \pm 11 \text{ kJ}\cdot\text{mol}^{-1}$), or even than fluorosulfuric acid ($\Delta H^0_{\text{acid}} = 1285 \pm 11 \text{ kJ}\cdot\text{mol}^{-1}$). Even more unexpectedly, a typical base such as ammonia becomes a stronger an acid than phosphoric acid ($\Delta H^0_{\text{acid}} = 1383 \pm 21 \text{ kJ}\cdot\text{mol}^{-1}$).²⁷ Similarly, 1H-tetrazole upon association with BeCl_2 , MgCl_2 and CaCl_2 is predicted to be a stronger acid in the gas phase than perchloric acid ($\Delta H^0_{\text{acid}} = 1255 \pm 24 \text{ kJ}\cdot\text{mol}^{-1}$).²⁷

Table 3. G4 binding enthalpies (D_0) of the complexes formed by association of the MH_2 and MF_2 ($M = \text{Be, Mg, Ca}$) derivatives with the deprotonated forms of NH_3 , H_2O , FH , PH_3 , SH_2 and ClH . The acidity enhancements ($\Delta\Delta H_{\text{acid}}$) of the corresponding neutral complexes $\text{MX}_2:\text{LB}$ ($M = \text{Be, Mg, Ca}$; $X = \text{H, Cl}$; $\text{LB} = \text{NH}_3, \text{H}_2\text{O}, \text{FH}, \text{PH}_3, \text{SH}_2, \text{ClH}$) are also included. All values in kJ mol^{-1} .

	D_0			$\Delta\Delta H_{\text{acid}}$		
	Be	Mg	Ca	Be	Mg	Ca
$\text{MH}_2\text{-NH}_2^-$	-349	-317	-345	254	240	258
$\text{MH}_2\text{-OH}^-$	-346	-320	-359	270	252	264
$\text{MH}_2\text{-F}^-$	- ^a	- ^a	- ^a	- ^a	- ^a	- ^a
$\text{MH}_2\text{-PH}_2^-$	-197	-199	-231	167	171	191
$\text{MH}_2\text{-SH}^-$	-210	-213	- ^a	177	182	- ^a
$\text{MH}_2\text{-Cl}^-$	-190	- ^a	- ^a	177	- ^a	- ^a
$\text{MCl}_2\text{-NH}_2^-$	-440	-416	-385	315	298	290
$\text{MCl}_2\text{-OH}^-$	-439	-417	-402	342	314	313
$\text{MCl}_2\text{-F}^-$	-424	-412	-394	387	349	322
$\text{MCl}_2\text{-PH}_2^-$	-267	-288	-266	222	233	219
$\text{MCl}_2\text{-SH}^-$	-278	-299	-285	233	240	234
$\text{MCl}_2\text{-Cl}^-$	-261	-292	-289	241	250	236

This acidity enhancement can be viewed as a direct consequence of the higher electron donor capacity of the deprotonated Lewis bases towards the MH_2 and MF_2 Lewis acids. Indeed, a comparison between the binding enthalpies of $\text{MX}_2:(\text{LB}_{\text{deprot}})^-$ into $\text{MX}_2 + (\text{LB}_{\text{deprot}})^-$ reported in Table 3 and the binding enthalpies of the neutral complexes $\text{MX}_2:\text{LB}$ into $\text{MX}_2 + \text{LB}$ reported in Table 1 reveals that the former are at least 3 times larger than the latter, leading to acidity enhancements never smaller than $170 \text{ kJ}\cdot\text{mol}^{-1}$. Actually, the acidity enhancement is directly related to the binding enthalpies of both the neutral and the anionic complexes, as deduced from the thermodynamic cycle shown in Scheme 1.



Scheme 1. Thermodynamic cycle relating the acidity of the isolated LBs and the LB:MX₂ complexes with the binding enthalpies of the LB:MX₂ aggregates and their deprotonated forms

Moreover, Figure 5 shows that although the acidity enhancement $\Delta\Delta\text{H}_{\text{acid}}^0$ is given by the difference between the two binding enthalpies, there is a very good linear correlation between $\Delta\Delta\text{H}_{\text{acid}}^0$ and the binding enthalpy of the anionic complex, $\text{D}_0((\text{LB}_{\text{deprot}})^-:\text{MX}_2)$, clearly indicating that this is the dominant contribution.

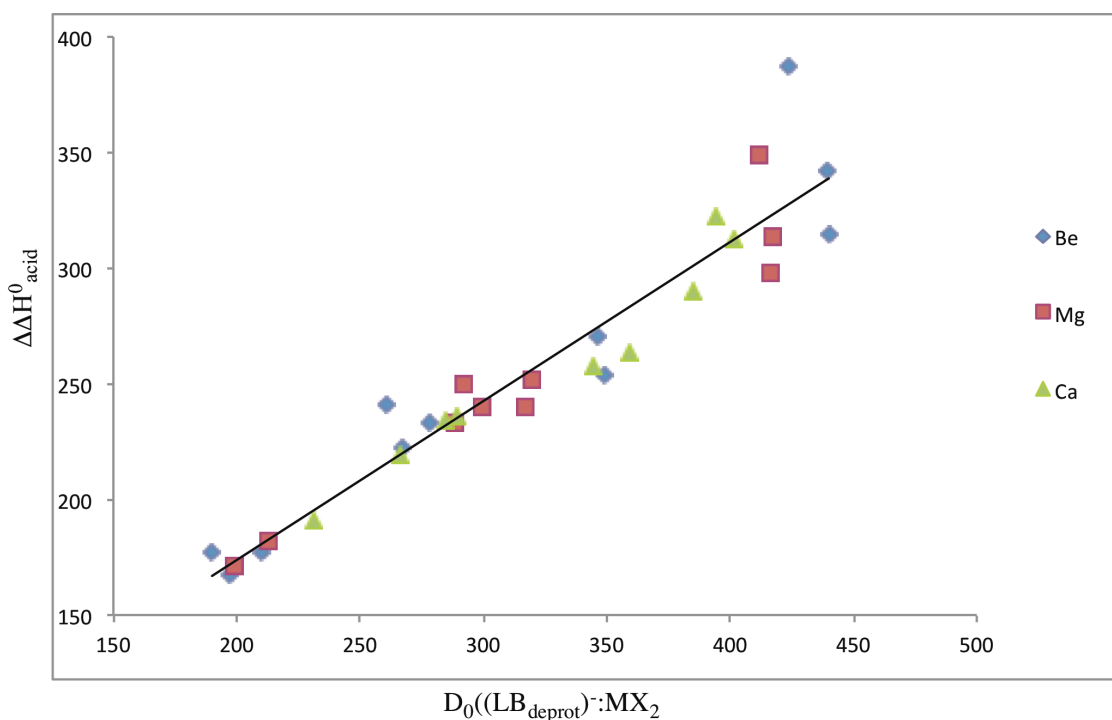


Figure 5. Linear correlation between the acidity enhancement of the LB:MX₂ (M = Be, Mg, Ca) complexes and the binding enthalpy of the anion obtained upon deprotonation. The linear correlation obeys the equation $\Delta\Delta\text{H}_{\text{acid}}^0 = 0.6876 \text{D}_0((\text{LB}_{\text{deprot}})^-:\text{MX}_2) + 36.288$, with $R^2 = 0.91$.

These results are consistent with the electron density redistributions of these complexes upon deprotonation. As shown in Figure 6a, the electron density at the BCPs of the Be-, Mg- and Ca-bonds significantly increases in a systematic manner from Be to Ca, whereas consistently the electron density at the M–F (M = Be, Mg, Ca) bonds decreases due to a larger electron donation from the NH_2^- moiety to the σ_{MF}^* antibonding orbital. Consistently, the M–N (M = Be, Mg, Ca) bonds significantly shorten upon deprotonation, whereas the M–F ones lengthen (see Figure 6b). Also, the larger charge transfer to the empty p orbital of the MF_2 (M = Be, Mg, Ca) subunit results in a smaller F–M–F bond angle around 120° , typical of a sp^2 hybridization.

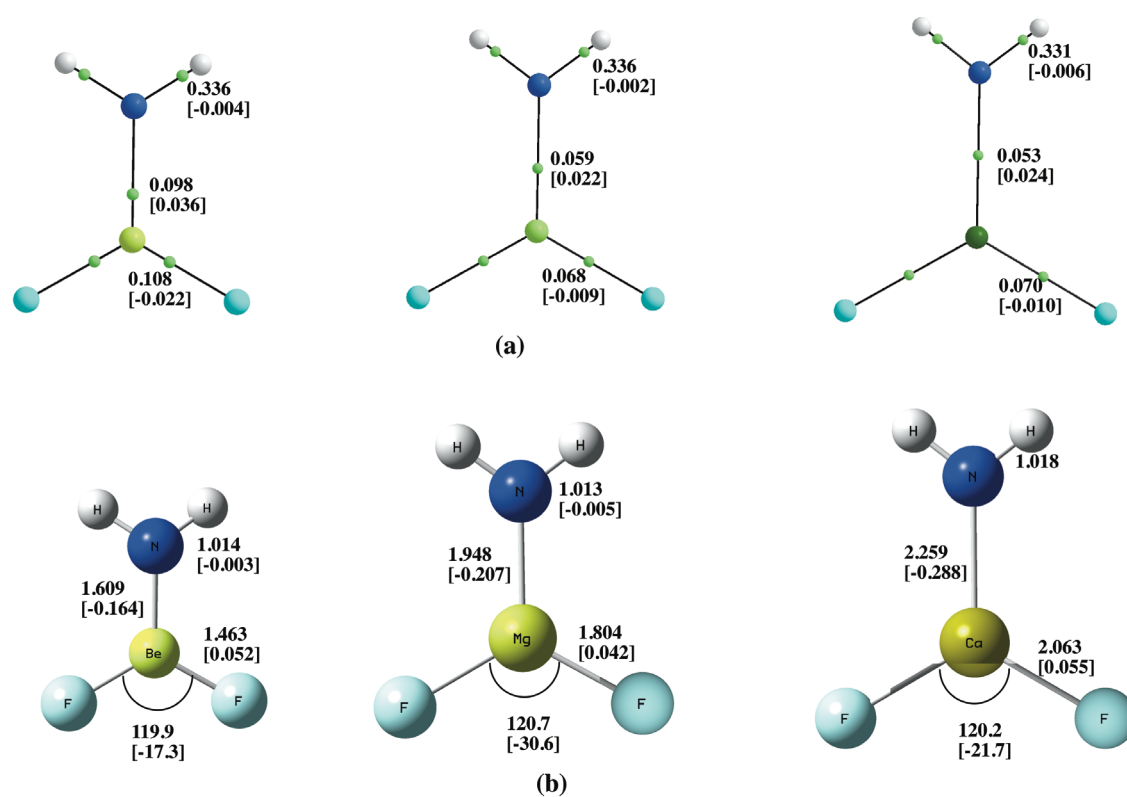


Figure 6. Complexes between MF_2 (M = Be, Mg, Ca) derivatives and NH_2^- . **(a)** Molecular graphs. Green denote BCPs. The electron densities at the BCPs are given in a.u.. The values within brackets show the changes in the density at the corresponding BCPs on going from the $\text{MF}_2:\text{NH}_3$ complex to its deprotonated form, $\text{MF}_2:\text{NH}_2^-$. **(b)** Optimized structures. Bond angles in degrees and bond lengths in Å. The values within brackets indicate the changes in bond lengths and bond angles on going from the $\text{MF}_2:\text{NH}_3$ complex to its deprotonated form, $\text{MF}_2:\text{NH}_2^-$.

It is also interesting to note that the acidity enhancements do not vary significantly with the nature of the alkaline-earth metal and, remarkably, the acidity enhancements triggered by beryllium derivatives are not necessarily the largest ones. This is indeed the most observed trend when the basic site of the Lewis base is a first-

row atom, but not when it is a second-row atom. In these latter cases, the acidity enhancement upon association with Mg derivatives is systematically slightly larger than with Be compounds, likely because the overlap of the lone-pair orbitals of a second-row base with the empty orbitals of another second row atom as Mg, is more efficient than with a first row element like Be.

4. Conclusions

We have shown that Mg and Ca derivatives are able to yield close-shell interactions with different Lewis bases of similar strength to the so-called beryllium-bonds. In all cases there is a significant electron density redistribution of both the Lewis base and the alkaline-earth derivative due to a significant charge transfer from the former toward the latter. As a consequence, the formation of the complexes is accompanied by a significant deformation of the interacting systems, which together with the appearance of secondary non-covalent interactions dictates the relative stabilities of the complexes formed. Hence, surprisingly, although Beryllium bonds were expected to be stronger than the Mg- and Ca-analogues, the dissociation of the latter into the two interacting units may require higher enthalpies than the dissociation of the Be-containing complexes. The aforementioned electron density redistributions are also reflected in dramatic changes of the reactivity of the interacting compounds, in particular on the intrinsic basicity of the Lewis bases investigated, to the point that conventional bases such as ammonia or aniline, upon complexation with MCl_2 ($M = Be, Mg, Ca$), become stronger Brønsted acids than phosphoric acid, whereas other bases such as 1H-tetrazole become stronger acids than perchloric acid. It is also important to emphasize that the possibility of modulating the intrinsic reactivity of many compounds through their participation in non-covalent interactions seems to be a rather general phenomenon. In this paper, we have found that this is the case for intrinsic acidities, but very recently it has been shown that also the basicity can be dramatically changed through the intervention of weak interactions.^{29,30}

Acknowledgments

This work was carried out with financial support from the Ministerio de Economía, Industria y Competitividad (projects CTQ2015-63997-C2 and CTQ2013-43698-P), by the COST Action CM1204 and Comunidad Autónoma de Madrid (S2013/MIT2841,

Fotocarbon). Thanks are also given to the CTI (CSIC) and the Centro de Computación Científica of the UAM (CCC-UAM) for their continued computational support.

References

- 1 L. Pauling *The nature of the chemical bond and the structure of molecules and crystals; an introduction to modern structural chemistry* 3rd. Ed. ed.; Cornell University Press: Ithaca (NY), 1960.
- 2 A. C. Legon *Phys. Chem. Chem. Phys.* 2017, **19**, 14884.
- 3 W. B. Yao; R. H. Crabtree *Inorg. Chem.* 1996, **35**, 3007.
- 4 I. Alkorta; J. Elguero; C. FocesFoces *Chem. Comm.* 1996, 1633.
- 5 T. Brinck; J. S. Murray; P. Politzer *Int. J. Quant. Chem.* 1992, 57.
- 6 I. Alkorta; I. Rozas; J. Elguero *J. Phys. Chem. A* 2001, **105**, 743.
- 7 S. J. Grabowski *Phys. Chem. Chem. Phys.* 2014, **16**, 1824.
- 8 A. Bauza; T. J. Mooibroek; A. Frontera *Angew. Chem. Int. Ed.* 2013, **52**, 12317.
- 9 G. Sanchez-Sanz; C. Trujillo; M. Solimannejad; I. Alkorta; J. Elguero *Phys. Chem. Chem. Phys.* 2013, **15**, 14310.
- 10 S. F. Vyboishchikov; G. Frenking *Theor. Chem. Acc.* 1999, **102**, 300.
- 11 P. Sanz; M. Yáñez; O. Mó *New J. Chem.* 2002, **26**, 1747.
- 12 L. M. Azofra; I. Alkorta; S. Scheiner *Phys. Chem. Chem. Phys.* 2014, **16**, 18974.
- 13 M. Yáñez; P. Sanz; O. Mó; I. Alkorta; J. Elguero *J. Chem. Theor. Comput.* 2009, **5**, 2763.
- 14 M. Yáñez; O. Mó; I. Alkorta; J. Elguero *Chem. Eur. J* 2013, **35**, 11637.
- 15 O. Mó; M. Yáñez; I. Alkorta; J. Elguero *Mol. Phys.* 2014, **112**, 592.
- 16 I. Alkorta; J. Elguero; O. Mó; M. Yáñez; J. E. Del Bene *Phys. Chem. Chem. Phys.* 2015, **17**, 2259.
- 17 O. Brea; I. Alkorta; O. Mó; M. Yáñez; J. Elguero; I. Corral *Angew. Chem. Eng. Int. Ed.* 2016, **55**, 8736.
- 18 O. Brea; I. Corral; O. Mó; M. Yáñez; I. Alkorta; J. Elguero *Chem. Eur. J.* 2016, **22**, 18322.
- 19 M. M. Montero-Campillo; I. Corral; O. Mó; M. Yáñez; I. Alkorta; J. Elguero *Phys. Chem. Chem. Phys.* 2017, **19**, 23052.
- 20 R. Tama; O. Mó; M. Yáñez; M. M. Montero-Campillo *Theor. Chem. Acc.* 2017, **136**.
- 21 L. A. Curtiss; P. C. Redfern; K. Raghavachari *J. Chem. Phys.* 2007, **126**, 12.
- 22 R. F. W. Bader *Atoms in Molecules. A Quantum Theory*; Clarendon Press: Oxford, 1990.
- 23 A. Savin; R. Nesper; S. Wengert; T. F. Fäsler *Angew. Chem. Int. Ed. Engl.* 1997, **36**, 1808.
- 24 A. Tood; T. K. Ketith In; Gristmill Software: Overland Park, KS: Overland Park KS, 2015.
- 25 S. Noury; X. Krokidis; F. Fuster; B. Silvi *Comput. & Chem.* 1999, **23**, 597.
- 26 E. R. Johnson; S. Keinan; P. Mori-Sánchez; J. Contreras-Garcia; A. J. Cohen; W. Yang *J. Am. Chem. Soc.* 2010, **132**, 6498.

- 27 J. E. Bartmess In *NIST Chemistry WeBook, NIST Standard Reference Database Number 69*; Linstrom, P. J., Mallard, W. G., Eds.; Institute of Standards and Technology: Gaithersburg MD, 20899, 2005.
- 28 K. M. Ervin; V. F. DeTuri *J. Phys. Chem. A* 2002, **106**, 9947.
- 29 C. Martín-Fernández; M. M. Montero-Campillo; I. Alkorta; J. Elguero *J. Phys. Chem. A* 2017, **121**, 7424.
- 30 C. Martín-Fernández; M. M. Montero-Campillo; I. Alkorta; M. Yáñez.; O. Mó; J. Elguero *Chem. Eur. J* 2017, (**in press**). DOI: 10.1002/chem.201705047